ABUAD Journal of Engineering Research and Development (AJERD)
ISSN (online): 2645-2685; ISSN (print): 2756-6811

Volume 7, Issue 2, 391-404

Investigation of the Fitness for Service (FFS) of Cracks in API 5L X70 Pipeline Steel using Failure Assessment Diagram (FAD)

Kingsley MUDJERE[1], Oyewole ADEDIPE[1], Asipita Salawu ABDULRAHMAN[2], Matthew Sunday ABOLARIN[1]

[1]*Department of Mechanical Engineering, Federal University of Technology, P.M.B 65, Minna, Niger State*
kmudjere@gmail.com/oye.adedipe@futminna.edu.ng/msabolarin2006@gmail.com

[2]*Department of Material and Metallurgical Engineering, Federal University of Technology, P.M.B 65, Minna, Niger State*
asipita.salawu@futminna.edu.ng

Corresponding Author: kmudjere@gmail.com, +2348063142473
Date Submitted: 13/03/2024
Date Accepted: 14/09/2024
Date Published: 26/09/2024

Abstract*: In this study, the fitness for service of crack propagation in API 5L X-70 stee1 was investigated using a model called Failure Assessment Diagram (FAD) to determine how fit a crack can be under certain operational pressure. It is a known fact that during the production of pipes, there are tendencies for flaws such as inclusions and cracks to occur in the pipes. When these flaws are subjected to stresses, there are tendencies for failures to occur starting from where the cracks or flaws are located. The failure due to the propagation of the cracks leads to oil spillage causing pollution to the environment which had negatively impacted livelihood of the host communities and aquatic lives. This had resulted in Government spending huge amount of money maintaining the pipelines and remediation. The purpose of this paper is to investigate the fitness for service of crack lengths 12 mm, 17 mm, 22 mm and 27 mm using the Failure Assessment Diagram (FAD) mode1. The material used in this paper is API 5L X 70 steel in the form of a Compact Tension (CT) specimen machined according to ASTM E1820 – 13. API 5L X-70 stee1 is a low-carbon stee1 with a carbon content of as low as 0.04 %. It is used in the production of pipelines for conveying crude oil and natural gas from the place of production to the place of refining or export. In the investigation of the fitness for service of the cracks, a charpy V-notch impact test was carried out to determine the energy required to fracture the steel, which was later inputted numerically into a critical stress intensity factor formula in accordance with BS 7910 – 13 standards to obtain the critical stress intensity factor (K_{IC} or K_Q). The stress intensity factor (K_I) was obtained from formula also according to BS 7910 – 13 standards. The ratio of K_I to K_Q was used in the FAD analysis. Subsequently, a monotonic tensile test was conducted to obtain the yield stress (σ_{ys}) and the reference stress (σ_{ref}) was obtained numerically according to BS 7910 – 13. The ratio of (σ_{ref}) to (σ_{ys}) was also used in the FAD analysis. The FAD analysis was used to determine the fitness for services and fracture behaviour of each crack. Scanning electron microscopy (SEM) was used to confirm the fracture behaviour obtained from the FAD. The results obtained show that the energy from the charpy V-notch impact test was 302.9 J and the critical stress intensity factor (K_Q) correlated numerically according to BS 7910 – 13 was determine as 246.73 MPa$\sqrt{m}$. The yield stresses obtained from the monotonic test for crack lengths of 12 mm, 17 mm, 22 mm and 27 mm were 132.51 MPa, 109.10 MPa, 114.36 MPa and 118.21 MPa, respectively. In the FAD analysis, it was observed that the safe operational stress to ensure fitness for service decreases with an increase in crack length. The fracture behaviour shows a ductile fracture behaviour since the FAD lies within the plastic collapse region. This fracture behaviour was confirmed by the image obtained from the scanning electron microscopy (SEM), which showed a cup and cone image suggesting ductile fracture behaviour. This FAD method will ensure that safe operational stresses are maintained for various crack length to prolong the life span of the pipeline. It is a novel method that can also be used to properly schedule the rate of inspection in pipelines alongside Ultrasonic sound, Liquid penetrant, Magnetic particle and radiographic methods of inspection.*

Keywords: *Failure Assessment Diagram, Yield Stress, Fracture Behaviour, Stress Intensity Factor, Reference Stress*

1. INTRODUCTION

The pipeline structures are used to transport petroleum and its products from the offshore point of production to the point of storage and possibly the point of export. Over the past 30 years, the world production of crude oil and gas and the consumption of their products have grown significantly, leading to an increase in the use of pipelines for their transport [1]. The American Petroleum Institute (API) classifies pipeline steels used in hydrocarbon production and transport environments as API 5LX steels [2]. The API 5L standards are used in the manufacture of steel pipelines for the transportation of oil and gas. The manufacturing of high-strength low-alloy (HSLA) steel through the process of thermo-mechanical treatment is to meet the need for high mechanical resistance, good fracture toughness at low temperatures and

good weldability. During operation, flaws in pipelines can initiate and propagate as fatigue cracks, as the structure is subjected to internal and external cyclic loading leading to fatigue failure in the pipelines.

One of the risks of damages in pipeline steel members is the presence of cracks, which may have occurred during the production of the pipeline, welding assembly or during operation. These cracks could appear as a result of the welding process, defects in the steel material, corrosion, or fatigue failure of steel members. The cost and losses associated with crack failure due to corrosion annually are approximately $300 billion or 3.2% of the GDP in the USA, 3 - 4% of GNP (Gross National Product) in Australia, Great Britain, Japan and other countries [3]. In a more recent publication, it was estimated that the global cost of corrosion stands at US$2.5 trillion, equivalent to roughly 3.4 percent of the global Gross Domestic Product (GDP) [4]. In Nigeria, a study was carried out on the losses and devastation caused by corrosion in the Nigerian oil industry for the past thirty-five (35) years. In the 35 years under review, it was found out that Nigeria has had about 7,359 incidences of oi1 spillage due to corrosion resulting in the release of 3,114,255 barre1 which was estimated at $247,957,000. This translated to an average of over 600 spills per annum, the highest rate of spills globally [5]. In China, a study was carried out where it was estimated that the cost of corrosion in China was approximate1y 2,127.8 billion RMB (~-310 bi11i0n USD), representing about 3.34% of the gross domestic product [6]. A research was carried out to evaluate the cost of corrosion in the crude oil processing industry. It was identified that corrosion is the major cost of production [7]. The principle of engineering economics and descriptive statistics were employed to determine the cost of corrosion per barrel and the annual value of corrosion cost, respectively. The result shows that the corrosion control cost per barrel stands at 77 cents per barrel. It was also observed that the use of chemical treatment as a means of preventing corrosion gave the highest cost of 81% of the total costs of prevention, while coating accounted for 19% of the total costs of prevention. Cathodic protection survey and crude analysis gave the lowest costs of 19% and 6%, respectively. It is imperative to know that offshore oil production and transport facilities contain many welds, and these welds may contain fabrication flaws or in-service cracks that can result in fatigue. In view, of these limitations, Engineering Critical Assessment (ECA) was developed to provide safe methods to determine the severity of defects in engineering structures. Therefore, fitness for service using the Failure Assessment Diagram (FAD) was developed.

2. LITERATURE REVIEW

There are limited reviews of literature in the failure assessment diagram (FAD) approach in ascertaining the fitness for service of cracks propagation in pipeline steel. In this study, the failure assessment diagram analysis is reviewed as well as the fundamental theory of fracture mechanics with particular interest in stress intensity factor of linear elastic fracture mechanics.

2.1 Failure Assessment Diagram (FAD)

Fai1ure Assessment Diagram (FAD) is a graphical procedure used to ascertain the fitness for services of operational metallic material. These materials, when produce cou1d be with an in-built defects or flaws and when in use, failure of the material can originate from the flaws [8]. The potential or actual cracks or defects in Engineering structures (Pipes, Beams among others) as enshrined in the UK Engineering Critical Assessment (ECA) is coded in two major document or standards called PD 6493 and CEGB R6 procedure. Failure Assessment Diagram (FAD) is one of the available method used to carry out Fitness for Service (FFS) assessment for pipelines and other Engineering structures. It helps to assess the safety of Structures component. This method is referred to as the two criteria method as it covers the behaviour of failures associated with plastic overloading (ductile fracture) and brittle fracture. To know if a crack may cause structural failure, the Failure Assessment Diagram (FAD) method is used [9]. In an elastic-plastic condition, failure assessment takes into account both brittle fracture and plastic deformation (ductile fracture). Both the ductile and brittle fractures are possible failure modes that are considered in Failure Assessment Diagram method. In pipelines, brittle fracture can occur suddenly and causes catastrophic results [10]. In the Failure Assessment Diagram (FAD) shown in Figure 1, k_r represents the brittle fracture ratio which is defined as the applied stress intensity factor divided by the material's toughness while L_r represents the load ratio which is defined as the reference stress divided by the lower yie1d strength of 0.2% proof stress.

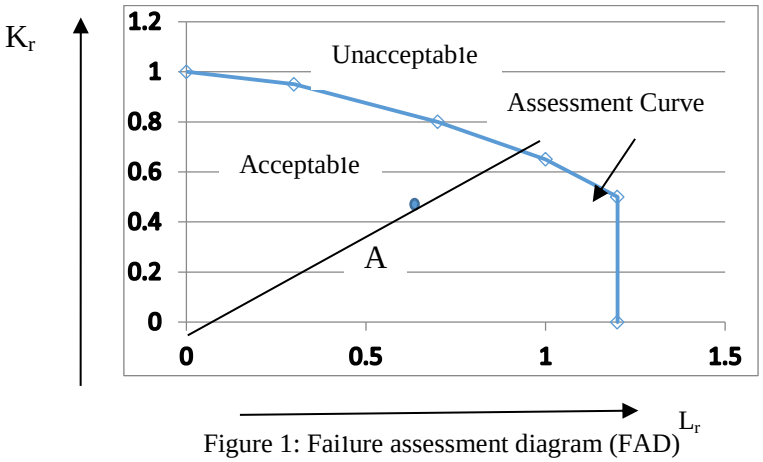

Figure 1: Fai1ure assessment diagram (FAD)

A Domain Failure Assessment Diagram DFAD is given in Figure 2; where the assessment point, A is given by the referral point with coordinate (Lr, Kr). In the FAD, the failure assessment curve shows us the safe and unsafe zones. The safe zone is divided in three conventional zones. If the assessment point, A is found in zone 1 where there is increase in pressure, brittle fracture occurs. In the zone 2, increase in applied pressure would cause elastic-plastic fracture to occur. In zone 3, plastic collapse occurs due to increased service pressure.

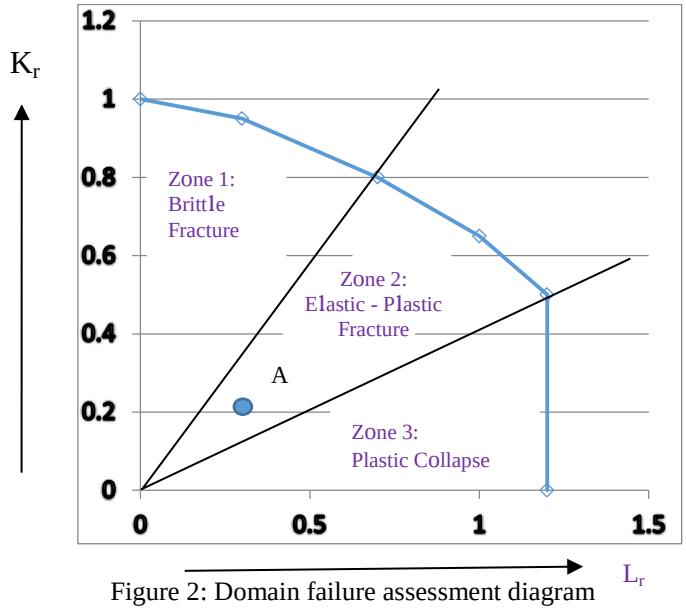

Figure 2: Domain failure assessment diagram

In FAD, the main focus is calculating stress intensity factor, K_I for different loading conditions and geometries. Finite element analysis, weight function and multiple reference state, can be used where stress intensity factor solution cannot be obtained from handbook. A combination of working load, transient thermal stresses, heat affected zone (HAZ), and residual stresses are considered to determine stress intensity factor, K_I that is used in FAD analysis [10]. However, the material data like fracture toughness, yield strength and the flow strength can be obtained from various standard test methods ([11]; [12]; [13]). It was shown that in FAD, the more ductile the material is, the more the calculated point will shift to the right and the more brittle the material is, the more the calculated point will shift to the left [10]. The standard reference point of maximum load ratio, L_{rmax} is 1.8 for stainless steels and 1.2 for carbon steels and this can be calculated from Equation 1.

$$L_{rmax} = (\sigma_{ys} + \sigma_{uts})/2\sigma_{ys} \quad (1)$$

A research was carried out using the Failure Assessment Diagram Method with Fatigue Crack Growth to Determine leak before Rupture, where a nozzle-cylindrical shell junction with a crack was considered and Abacus standard was used to compute elastic-plastic J- integral results along the crack front [9]. The obtained results were further used to calculate the plastic collapse reference stress that was used to obtain the plastic collapse ratio ($L_r = \sigma_{ref}/\sigma_{ys}$) and elastic analysis was used to obtain the stress intensity factor that was used to obtain brittle fracture ratio ($K_r = K_I/K_Q$) then these ratios gave the location of the evaluated point on the FAD to indicate structural failure or safety.

2.2 Calculating Safety Factor in FAD

Figure 3 shows the presentation of how safety factor or load factor in failure Assessment Diagram (FAD) is calculated. The safety factor in Failure Assessment Diagram (FAD) as stated by [14] is as shown in Equation 2;

$$F_s = \frac{0D}{0B} \quad (2)$$

where F_s is the safety factor. The advantage of using safety factor, F_s was stated by [14] as follow;

1. It serves as a unique too1 for defining the safe zone.
2. It is used as so1ution for non-critica1 zone

2.3 Theoretical Fundamentals of Fracture Mechanics

Fracture Mechanics is the field of mechanics concerned with the study of the propagation of cracks in material. It uses methods of analytical and numerical solid mechanics to calculate the driving force on a crack and those of experimental solid mechanics to characterize the material resistance to fracture. Fracture mechanics was defined as an important specialization in solid mechanics where the presence of a crack is assumed and the quantitative relationship between crack

length, the material resistance to crack growth and the stress at which the crack propagates at high speed is determined to cause structural fracture [15]. The field of fracture mechanics has over the years prevented numerous amount of structural failure that could have led to serious destructions of live and properties but this can hardly be quantified because it is not possible to quantify the disasters that do not happen [16]. There is the need to understudy the basic approach in fracture mechanics for better understanding of the principle of fracture mechanics.

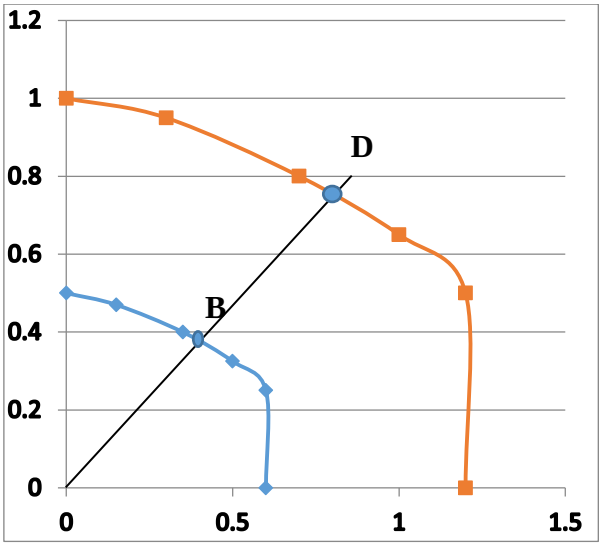

Figure 3: Calculation of safety factor in FAD

2.3.1 Linear elastic fracture mechanics

Linear Elastic Mechanics is concerned with predicting conditions that give rise to rapid crack growth in brittle materials that are considered to be elastic, homogeneous and isotopic at the onset of fracture. Linear elastic fracture mechanics (LEFM) is only valid as long as nonlinear material deformation is confined to a small region surrounding the crack tip [16].

i. **The stress intensity factor approach:** This approach explains stress states close to the tip of the sharp crack and this is the approach that is frequently used in engineering practices. Stress intensity factor in a homogenous linear elastic body is defined as the magnitude of elastic stress field singularity [10]. It was further explained that stress intensity factor (SIF) has a relationship with crack length, applied force and specimen geometry. In understanding the stress intensity approach, one can say that it describes the stress field at the tip of the crack. It is worthy of note that every steel material has its own fracture toughness also refers to as the critical fracture toughness usually represented as K_{Ic} or the material fracture toughness, K_Q, while the stress intensity factor is represented as K. The relationship between stress intensity factor, K and the critical stress intensity factor, K_{Ic} or K_Q can be likened to the relationship between stress, σ and yield stress, σ_{ys} respectively. For better understanding of the stress intensity factor approach, it was explained that in investigating crack in any structure under any loading condition, the stress intensity factor, K has to be determined and used to measure the fracture toughness of the material. In other words, K_{Ic} or K_Q is the bench mark to understand whether the structure will fail due to the existing crack in the structure [10]. The critical stress intensity factor, K_{Ic} for Plain Carbon Ferritic Steel (API 5LX70) is put at 197 MPa$\sqrt{m}$. (Marchi & Somerday, 2023). It was explained that, if it is assumed that a material fails at some critical stress or strain combination, and then fracture must occur at a critical stress intensity factor, K_{Ic} [16]. He further stated that K_{Ic} is an alternative measure of fracture toughness. The principle of stress intensity factor can as well be likened to the explanation that when a stress magnitude of a body gets to its yield strength, the body plastically deforms and cannot return to its original elastic position again. In the same way, when the stress intensity factor, K reaches the critical fracture toughness, K_{Ic} or K_Q, the cracked structure fractures or fails completely. In this theoretical background, fracture mechanics is based on the stress distribution at the tip of the crack derived from elasticity theory. In this theory, there are three types of crack mode with each mode of loading producing $1/(r)^{1/2}$ singularity at the tip of the crack where each mode depends on the proportionality constant k and f_{ij}. The crack tip conditions are defined by stress intensity factor because all stresses, strains and displacement can be so1ved with the value of K_I. The stresses close to the crack tip increases in direct proportion to K_I, K_I been responsible for the amplitude of the crack tip singularity. K_I is a function of loading condition, crack size and shape, and other geometric parameters [17]. Therefore, K_I can be defined by the expression in Equation 3.

$$K_I = Y\sigma\sqrt{\pi a} \quad (3)$$

Where,

σ_o is the stress applied remotely,
a is the crack length.
Y is the geometric factor, which is a dimensionless constant that depend on crack geometry and mode of loading.
A1so, K_I can be defined by the expression in Equation 4 [18]

$$K_I = C\sigma\sqrt{\pi a} \quad (4)$$

Where, $C = (1 - 0.1\eta^2 + 0.96\eta^4)\sqrt{(1/cos\pi\eta)}$ (5)

$\eta = a/b$ (6)

$a =$ Crack 1ength

$b =$ Width of the steel sheet

A1so, K_I can be defined by the expression in Equation 7. [16]

$$K_I = \sigma\sqrt{\pi a} \quad (7)$$

This study is to investigate the fitness for service of the cracks in the selected pipeline steel using the failure assessment diagram method. The failure assessment diagram (FAD) method will help to schedule the rate of inspections that will be carried out on the pipeline to quickly arrest any catastrophic failure in the pipeline that will results in leakages of petroleum products that can cause pollution to the environment. This is a novel way of ensuring that crack propagation in the pipeline is monitored to avoid sudden failure as against the conventional methods of inspection such as ultrasonic sound, radiographic, magnetic particle and liquid penetrant method.

3. MATERIAL AND METHODS

The material used in this research work is the API 5L X 70 steel that is commonly used in the production of pipeline steels. The methods used in the research consists of series of tests which include designing the compact tensile (CT) specimen upon which the following tests were carried out: optica1 Emission Spectroscopy (OES) to ascertain the chemical composition of the material; Charpy V-notch impact test to determine the energy required to numerically calculate the critical stress intensity factor (K_Q or K_{IC}); the stress intensity factor (K_I) was numerically calculated according to BS 7910 – 13 standard; monotonic tensile test to determine the yield stress (σ_{ys}) and the reference stress (σ_{ref}) was numerically calculated according to BS 7910 – 13 standard. Then the ratio of K_I to K_Q and the ratio of σ_{ref} to σ_{ys} was used to develop the FAD and to assess the fitness for service of the various crack lengths created on the CT specimen.

3.1 Material

The most predominant materials used as pipeline materials before the 1980s are mostly cast iron and steel [19]. In this article, the API 5L X70 Steel which is a low carbon steel was used.

3.1.1 Chemical composition of base material

The chemical characterisation of the base material (API 5LX70) was determined using optical Emission Spectroscopy (OES) as shown in Figure 5.

3.2 Methods

In this article, the specimen used is the compact tensile (CT) specimen. The specimen for fracture toughness test was design in accordance with ASTM E1820 - 13 Standard [20]. In this standard, the thickness of the specimen is the most important factor that affect the resultant fracture toughness or stress intensity factor. The thickness is determined according to ASTM E1820 -13 as shown in Equation 8:

$$B \geq 2.5(K_Q/\sigma_{ys})\text{^}2 \quad (8)$$

Where: B is the thickness of the specimen, K_Q is the fracture toughness, σ_{ys} is the yield strength of the material. In this article the thickness considered is 12 mm as seen in Figure 4.

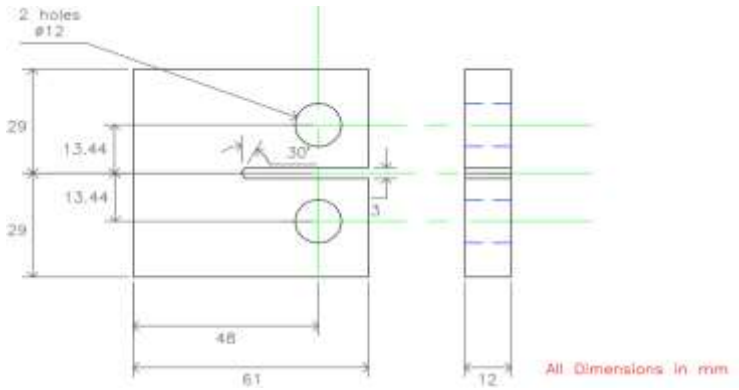

Figure 4**:** Design of compact tension specimen

3.2.1 Production of CT specimen

All the test specimens were produced by specialist mechanical technicians and machined to the ASTME1820 standard. The CT specimens that were produced were four in number with each having crack length of 12 mm, 17 mm, 22 mm and 27 mm. The cracks were created horizontally through a pre-crack using the straight through notch fatigue crack starter method. Experience has shown that it is not practicable to obtain a sharp narrow matched notch that will simulate a natural crack which will produce a satisfactory fracture toughness test result [21].

3.3 Experimental Procedures and Laboratory Test

The methodology used in the research is test methods which consist of optical Emission Spectroscopy (OES), monotonic tensile test, Charpy V-notch impact test and then the development of the failure assessment diagram (FAD) to assess the fitness for service for each of the crack length 12 mm, 17 mm, 22 mm and 27 mm.

3.3.1 Optical emission spectroscopy (OES) test

The chemica1 composition of API 5LX70 used in this research work was determined using optical Emission Spectroscopy (OES) as shown in Figure 5 to ascertain its present characteristics. Optical emission spectroscopy (OES) is a method of Positive Material Identification (PMI) that creates a spark on the sample in the presence of argon gas. The Positive Material Identification (PMI) is the analysis of metallic alloys or any other materials to establish their composition by reading the quantities by percentage of their constituent elements. In the parent material, three sparks were created to determine the accurate composition of the material. The spark created was used to excite the atoms within the sample material and these excited atoms emitted light at specific frequencies which are then used to precisely determine the composition of the steel. In creating the sparks, the argon gas in an argon bottle was ensured to be sufficient and that the argon flow was set at 8 litres per minute. A calibration process was carried out for all elements as per the requirement of the specification with the use of a standard calibration test blocks. Thereafter, the test specimen was sand papered using a 60 grit sand paper to ensure a better levelling and touching the surface was avoided to prevent contamination of the prepared surface. On completing the preparatory process, the sample was place on a spark stands and the spark created via a computer command. This spark process analysis was repeated on the same sample three times and the test resu1ts appear on the computer and the element appeared in percentages.

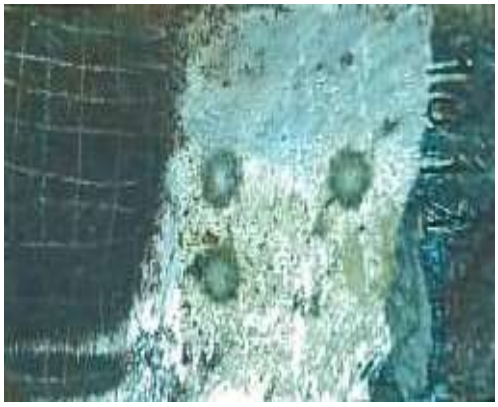

Figure 5: Spectroscopic analysis of parent steel

3.3.2 Charpy V – notch impact test

The charpy V – notch impact tester was used to evaluate the energy required to break parent metal. The parent API 5LX70 steel of dimension 10 mm x 10 mm x 10 mm was used and a V-notch of 2 mm was created in the parent metal as shown Figure 6. Thereafter, the V- notch steel was placed on the breaking centre pin of the charpy V - notch impact tester using a special plier of the same temperature as the specimen. The load or the pendulum was released on it to break it through the V-notch created after ensuring that the safety door was closed to avoid the broken specimen flying out to injure somebody. The broken parent specimen resulting from charpy V - notch impact test is shown in Figure 7. On completion of the test, the pendulum returns back to its locking position and the test in joules required to break the parent steel was taken from the computer and recorded and an average reading taken.

3.3.3 Fracture toughness test using monotonic approach

Four (4) parent specimens were used to carry out the fracture toughness test in air. These four (4) parent specimens include one control specimen which has a V – notch of length 10 mm plus crack length of 12 m making a total crack length of 22 mm, (a/w) = 0.460 and $f(\frac{a}{w})$ = 8.58 [22] that enables a valid fracture toughness and three (3) specimens with pre-crack of 5 mm, 10 mm and 15 mm. The specimens were all fractured monotonically in air using the universal tensile machine (UTM). Thereafter, the fractured surfaces were examined using Scanning Electron Microscopy (SEM) to ascertain the fracture behaviour of the four (4) parent metal in air after which a failure assessment diagram (FAD) ana1ysis was conducted to ascertain it fitness for service.

Figure 6: Parent meta1 V – Notched specimen

Figure 7: Broken parent specimen resulting from Charpy V- Notch test

3.3.4 Developing failure assessment diagram (FAD) for the research

In developing the failure assessment diagram (FAD), the first thing that was considered was the determination of the mechanical properties such as yield strength and ultimate tensile strength of the parent steel. Thereafter, the energy required to break the charpy V - notch specimen stated in charpy V - notch impact test in paragraph 2.3.2 was recorded and the average value was recorded. The critical stress intensity factor (CSIF) was obtained from the relationship between energy in Joules, thickness of the specimen and critical stress intensity factor as shown in Equation 9

$$\mathrm{KQ} = \mathrm{K_{Ic}} = [(12\sqrt{C_v} - 20)(25/B)^{0.25}] + 20 \quad (9)$$

Where;
K_{Ic} is the estimate of the critical fracture toughness in MPa$\sqrt{m}$
B is the thickness of the material for which an estimate of K_{Ic} was required in mm
C_v is the lower bound charpy V-notch impact energy at the service temperature in Joules (J) [8].
After obtaining the critical stress intensity factor, the load required to initiate crack was evaluated from Equations 10 and 11

$$K_Q = [(P_Q)/BW^{1/2}]f(\frac{a}{W}) \quad (10)$$

Where K_Q is the Critica1 Stress Intensity Factor.

$$f\left(\frac{a}{W}\right) = \frac{\left(2+\frac{a}{W}\right)\left[0.886+4.64\left(\frac{a}{W}\right)-13.32\left(\frac{a}{W}\right)^2+14.72\left(\frac{a}{W}\right)^3-5.6\left(\frac{a}{W}\right)^4\right]}{\left(1-\frac{a}{W}\right)^{1.5}} \quad (11)$$

Where, B is the thickness of the specimen, a is the crack length, W is the width of the specimen, P_Q is the load required to initiate crack.

The brittle fracture ratio and the plastic collapse ratio that was used in the failure assessment diagram (FAD) were obtained using the Equations 12 and 13.

$$Kr = \frac{KI}{KQ} \quad (12)$$

$$Lr = \frac{\sigma ref}{\sigma ys} \quad (13)$$

The reference stress was obtained using Equations 14 and 15.

$$\sigma_{ref} = [P_b + [P_b^2 + 9P_m^2]^{0.5}]/3[1-\propto^{"}] \quad (14)$$

Where,

$$\propto^{"} = a/w \quad (15)$$

P_b is the bending stress
P_m is the hop membrane stress
The actua1 reference stress that was used was the reduce reference stress since there is no bending stress, the Equation 14 was reduced to Equation 16.

$$\sigma_{ref} = [9P_m^2]^{0.5}]/3[1-\propto^{"}] \quad (16)$$

The stress intensity factor that was used in the failure assessment diagram (FAD) was determined using Equations 17, 18 and 19.

$$K_I = C\sigma\sqrt{\pi a} \quad (17)$$

Where, $C = (1 - 0.1\eta^2 + 0.96\eta^4)\sqrt{(1/cos\pi\eta)}$ (18)

$$\eta = a/b \quad (19)$$

a = Crack length
b = Width of the steel sheet

The failure assessment diagram (FAD) curve is used to assess whether a crack is fit for service or not. The crack is considered fit for service, if the point under consideration falls within the curve but it is considered not fit for service, if the point under consideration falls outside the curve. This curve can be generated using different options depending on certain conditions. In developing the FAD assessment curve, according to BS 7910-13, Equations 20 to 29 were used to generate the points for the curve.

$$f(Lr) = [1 + 0.5(Lr^2)^{-0.5}]\,[0.3 + 0.7\exp(-\mu Lr^6)] \text{ for } Lr \leq 1 \quad (20)$$

$$f(Lr) = f(1)Lr^{N-1/2N} \text{ for } 1 < L_r < L_{r,Max} \quad (21)$$

$$f(L_r) = 0 \text{ for } L_r \geq L_{r,Max} \quad (22)$$

where

$$\mu = \min[0.001(E/\sigma_y), 0.6] \quad (23)$$

$$N = 0.3[1 - (\sigma_y/\sigma_u)] \quad (24)$$

For materials that exhibit yield discontinuity,

$$f(Lr) = [1 + 0.5(Lr^2)^{-0.5}] \text{ for } Lr < 1 \quad (25)$$

$$f(Lr) = [\lambda + (2\lambda)^{-1}]^{-0.5} \text{ for } L_r = 1 \quad (26)$$

Where;

$$\lambda = \left[1 + \left(\frac{E\Delta\varepsilon}{Re1}\right)\right] \quad (27)$$

$$\Delta\varepsilon = 0.0375(1 - 0.001\sigma_y) \text{ for } \sigma_y \leq 1000 \quad (28)$$

$$Re1 < 946\text{MPa}. \quad (29)$$

Where E is the young modulus, σ_y is the yield strength and σ_u is the ultimate tensile strength.

3.3.5 Scanning electron microscopy (SEM)

All samples must be of an appropriate size to fit in the specimen chamber and are generally mounted rigidly on a specimen holder called a specimen stub. Several models of SEM can examine any part of a 6-inch (15 cm) semi-conductor wafer, and some can tilt an object of that size to 45^0. Samples are coated with platinum coating of electrically conducting material, deposited on the sample either by low-vacuum sputter coating or by high-vacuum evaporation. SEM instruments place the specimen in a relative high-pressure chamber where the working distance is short and the electron optical column is differentially pumped to keep vacuum adequately low at the electron gun. The high-pressure region around the sample in the ESEM neutralizes charge and provides an amplification of the secondary electron signal. Low-voltage SEM is typically conducted in an FEG-SEM because the field emission guns (FEG) is capable of producing high primary electron brightness and small spot size even at low accelerating potentials. Embedding in a resin with further polishing to a mirror-like finish can be used for both biological and materials specimens when imaging in backscattered electrons or when doing quantitative X-rays micro-ana1ysis.

4. RESULTS AND DISCUSSION

The values of the critical stress intensity factor (K_Q), the stress intensity factor (K_I), the reference stress (σ_{ref}) and the yield stress (σ_{ys}) obtained from the entire test and calculations were used to analyse the failure assessment diagram (FAD). Thereafter, the fracture behaviour of each crack was examined under SEM and compared with the ones obtained from the FAD as shown in Figure 8 and Figure 9. In assessing the fitness for service of the various crack lengths, the pressures being operated at the particular crack length are relatively stable and serve as the safe operational stresses that are required to safely operate the pipeline system with the particular crack length without catastrophic failure thereby prolonging the life span of the pipeline.

4.1 Results obtained from the Materials Chemical Composition Test

The results obtained from the optical Electron Spectroscopy (OES) are as shown in Table 1. From Table 1, it can be seen that iron content of the specimen is 97.709%, 0.003%N, 0.04%C, 0.003%Zr and traces of other elements.

Tab1e 1: Typical chemical composition of API 5LX70 carbon stee1

E1em	C	Mn	Si	P	S	Cr	Mo	Ni	Nb	A1	Cu	V
Comp wt %	0.04	1.55	0.15	0.01	0.002	0.224	0.131	<0.002	0.054	0.03	0.007	0.03

Co	B	Ti	W	Mg	Ca	Ce	1a	As	Pb	Sn	Sb
<0.002	0.00005	0.019	<0.005	0.0013	0.0031	<0.002	0.006	<0.005	0.011	<0.001	0.012

Te	Zn	Zr	N	Fe
<0.001	<0.001	0.003	<0.003	97.709

4.2 Results obtained from Charpy V – Notch Impact Test

Tab1e 2 shows the results of the charpy V-notch impact test for three different parent metals. It can be seen that the impact energy of the specimen under similar condition are in proximity with specimen P 360 body (1) offering the least resilience.

Tab1e 2: Charpy V-Notch impact energy results for parent metal

Code Specimen	Width (mm)	Thickness (mm)	Section (mm^2)	Energy (J)	Resilience (J/cm)	Sheer (%)	LE (MM)
P 390 Body (1)	10	10	80	297.9	372.375	100	2
P 390 Body (2)	10	10	80	300.5	375.625	100	2.1
P 390 Body (3)	10	10	80	310.2	387.75	100	2.1

Table 3 shows the statistical values using the three values obtained from the charpy V-notch energy results to obtain the mean value, standard deviation, minimum value, maximum value and the range. The mean value of the energy released is the value of the energy that is required to obtain the critical stress intensity factor in the correlation relationship in Equation 9.

Tab1e 3: Statistical values of charpy V-Notch impact energy results for parent metal

	Energy (J)	Resilience (J/cm)
Mean Value	302.9	378.58333
Standard Deviation	5.3	6.61622
Minimun Values	297.9	372.375
Maximum Values	310.2	387.75
Range	12.3	15.375

The result of the critical stress intensity factor obtained from the correlation relationship between the energy obtained from charpy V-notch impact test, specimen thickness and the critical stress intensity factor in Equation 9 is shown in Tab1e 4. This critical stress intensity factor is required in the development of the failure assessment diagram (FAD) points that will be used to ascertain the fitness for service of each crack lengths.

Table 4: Critical stress intensity factors for parent API 5LX70 steel

	Critical Stress Intensity Factor (K_Q) ($MPa\sqrt{m}$)
Parent Meta1	246.73

4.3 Results obtained from Monotonic Tensile Test

The results obtained from monotonic tensile test are presented in Table 5. From the results, it can be seen that the specimen with the least crack length has the highest tensile strength, this can be specimen with higher crack length offers least resistance to failure and there is higher tendency for failure to propagate at a higher crack length.

Tab1e 5: Stress results for parent API 5LX70 in air

Crack Length (mm)	Tensi1e Stress (Mpa)	Yie1d Stress (Mpa)
12	132.51	132.51
17	109.10	109.10
22	117.35	114.36
27	118.21	118.21

4.4 Results obtained from Scanning Electron Microscopy (SEM)

The SEM results simply show that the fracture behaviour of the API 5LX70 stee1 is a ductile fracture which can be seen from the cup and cone features in the image shown in Figure 8. The network of cup-and-cone style ridges and dips also called the micro-void coalescence suggested that a ductile fracture took place. This micro-void coalescence occurs when voids are formed around tiny inclusions in the steel as it stretches open during yielding. These micro-void coalescences eventually combine together to create larger voids which eventually causes fracture. When this stable ductile crack extension is viewed under the microscope, micro-void coalescence is identified as the failure mechanism.

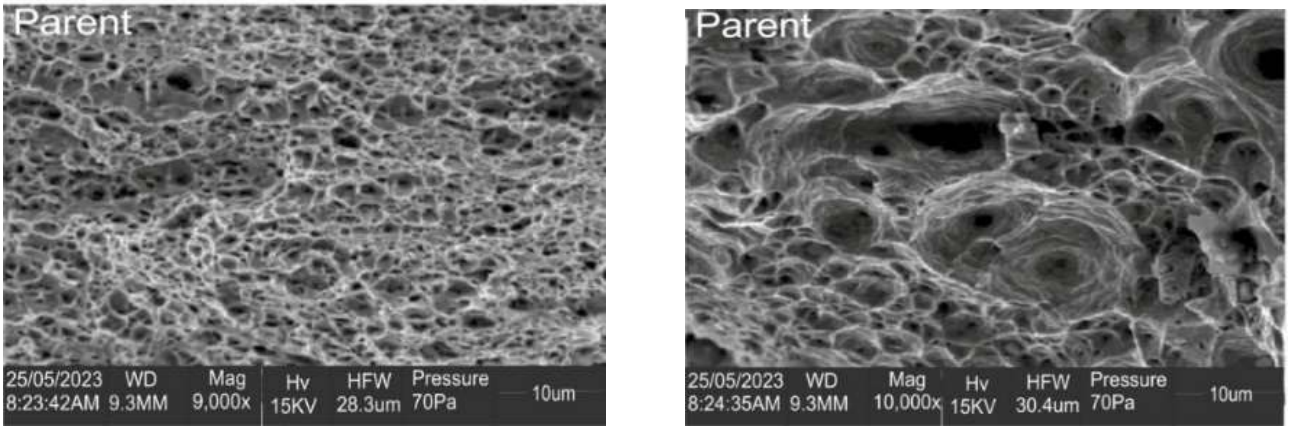

(a) **(b)**

Figure 8: Scanning electron microscopy (SEM) result for fractured parent stee1 showing (a) 9,000x magnification and (b) 10,000x magnification

4.5 Failure Assessment Diagram (FAD) Analysis of Fitness for Service in Air

In comparing the results obtained from the Failure Assessment Diagram (FAD) in Figure 9, Tables 6, Table 7, Table 8 and Table 9 with the fracture of parent steel with crack length 12 mm, 17 mm, 22 mm and 27 mm in air in Table 5, it was observed that for parent steel of crack length 12 mm, the safe operational stresses range from 2.5 MPa to 80 MPa where the crack is stable and failure actually started from 90 MPa. The safe operational stresses for crack length 17 mm range from 2.5 MPa to 50 MPa where the crack is stable and failure actually started from 60 MPa. The safe operationa1 stresses for crack length 22 mm range from 2.5 MPa to 40 MPa where the crack is stable and failure actually started from 50 MPa. The safe operational stresses for crack length 27 mm range from 7.5 MPa to 30 MPa where the crack is stable and failure actually started from 40 MPa. The tensile stresses responsible for fracture monotonically in the parent steel in air as shown in Figure 5 are 132.51 MPa, 109.10 MPa, 117.35 MPa and 118.21 MPa for 12 mm, 17 mm, 22 mm and 27 mm crack lengths respectively but the fractures actually took place at 90 MPa, 60 MPa, 50 MPa and 40 MPa for crack lengths 12 mm, 17 mm, 22 mm and 27 mm respectively according to the result obtained from failure assessment diagram (FAD). The results suggested that failure actually started taking place within the material bef0re the physical failure that can be seen with the physical sees, this is evident for crack length 12 mm, where the tensile stress is 132.51 MPa but failure actually occurred at 90 MPa. For crack length 17 mm, the tensile stress is 109.10 MPa but failure actually occurred at 60 MPa. For crack length 22 mm, the tensile stress is 117.35 MPa but failure actually occurred at 50 MPa. For crack length 27 mm, the tensile stress is 118.21 MPa but failure actually occurred at 40 MPa. The results also show that the safe operational stresses decrease with increase in crack length. Also, in Figure 9, it was observed that all the crack lengths fall within the plastic collapse zone which suggested that the fracture is a ductile fracture behaviour which confirms the ductile fracture behaviour shown in the SEM image in Figure 8. It was a1so observed that the crack length 12 mm is less ductile than the crack length 17 mm, crack length 17 mm is less ductile than the crack length 22 mm and crack length 22 mm is less ductile than the crack length 27 mm. This can be seen in the FAD in Figure 9, where crack length 12 mm tends towards the elastic-plastic fracture zone followed by the crack length 17 mm, crack length 22 mm and crack length 27 mm.

Tab1e 6: Fitness for services of parent crack length 12mm using failure assessment diagram (FAD)

Crack Length (mm)	Stress, σ (Mpa)	Ref. Stress, σref (Mpa)	Stress Intensity Factor (SIF), K_I (MPa√m)	Yield Stress, σys (Mpa)	Critical Stress Intensity Factor, KIC (MPa√m)	Kr	Lr	load Factor or Factor of Safety	Crack Status
12	2.5	4.62	0.66	132.51	246.73	0.0026	0.0349	34.370	Stab1e
12	10	18.46	2.62	132.51	246.73	0.0106	0.1393	8.611	Stab1e
12	20	36.92	5.24	132.51	246.73	0.0212	0.2786	4.306	Stab1e
12	30	55.38	7.87	132.51	246.73	0.0319	0.4179	2.870	Stab1e
12	40	73.85	10.49	132.51	246.73	0.0425	0.5573	2.152	Stab1e
12	50	92.31	13.11	132.51	246.73	0.0531	0.6966	1.722	Stab1e
12	60	110.77	15.73	132.51	246.73	0.0638	0.8359	1.435	Stab1e
12	70	129.23	18.36	132.51	246.73	0.0744	0.9752	1.230	Stab1e
12	80	147.69	20.98	132.51	246.73	0.0850	1.1146	1.076	Stab1e
12	90	166.15	23.60	132.51	246.73	0.0957	1.2539	0.957	Fai1ure

Initiation Point (Lr , Kr) = (1.2 , 0.085)
Initiation Load Factor 0r Safety Factor = 1.0

Tab1e 7: Fitness for services of parent crack length 17mm using failure assessment diagram (FAD)

Crack Length (mm)	Stress, σ (Mpa)	Ref. Stress, σref (Mpa)	Stress Intensity Factor (SIF), K_I (MPa√m)	Yield Stress, σys (Mpa)	Critical Stress Intensity Factor, KIC (MPa√m)	Kr	1r	Load Factor or Factor of Safety	Crack Status
17	2.5	5.71	0.73	109.10	246.73	0.0030	0.0523	22.946	Stab1e
17	10	22.86	2.91	109.10	246.73	0.0118	0.2095	5.729	Stab1e
17	20	45.71	5.81	109.10	246.73	0.0235	0.4190	2.864	Stab1e
17	30	68.57	8.72	109.10	246.73	0.0353	0.6285	1.910	Stab1e
17	40	91.43	11.63	109.10	246.73	0.0471	0.838	1.432	Stab1e
17	50	114.29	14.53	109.10	246.73	0.0589	1.0476	1.146	Stab1e
17	60	137.14	17.44	109.10	246.73	0.0707	1.2570	0.955	Fai1ure
17	70	160.00	20.35	109.10	246.73	0.0825	1.4665	0.818	Fai1ure
17	80	182.86	23.25	109.10	246.73	0.0942	1.6761	0.716	Fai1ure
17	90	205.71	26.16	109.10	246.73	0.1060	1.8855	0.637	Fai1ure

Initiation Point (Lr, Kr) = (1.2, 0.07)

Initiation Load Factor or Safety Factor = 1.0

Table 8: Fitness for services of parent crack length 22 mm using failure assessment diagram (FAD)

Crack Length (mm)	Stress, σ (Mpa)	Ref. Stress, σref (Mpa)	Stress Intensity Factor (SIF), K_I (MPa√m)	Yield Stress, σys (Mpa)	Critical Stress Intensity Factor, K_{IC} (MPa√m)	Kr	1r	Load Factor or Factor of Safety	Crack Status
22	2.5	7.50	0.79	114.36	246.73	0.0032	0.0656	18.294	Stable
22	10	30.00	3.17	114.36	246.73	0.0128	0.2623	4.575	Stable
22	20	60.00	6.34	114.36	246.73	0.0257	0.5247	2.287	Stable
22	30	90.00	9.51	114.36	246.73	0.0385	0.7870	1.525	Stable
22	40	120.00	12.69	114.36	246.73	0.0514	1.0493	1.144	Stable
22	50	150.00	15.86	114.36	246.73	0.0643	1.3116	0.915	Failure
22	60	180.00	19.03	114.36	246.73	0.0771	1.5740	0.762	Failure
22	70	210.00	22.20	114.36	246.73	0.0900	1.8363	0.654	Failure
22	80	240.00	25.37	114.36	246.73	0.1028	2.0986	0.572	Failure
22	90	270.00	28.54	114.36	246.73	0.1157	2.3610	0.508	Failure

Initiation Point (Lr , Kr) = (1.2 , 0.06)

Initiation Load Factor or Safety Factor = 1.0

Table 9: Fitness for services of parent crack length 27 mm using failure assessment diagram (FAD)

Crack Length (mm)	Stress, σ (Mpa)	Ref. Stress, σref (Mpa)	Stress Intensity Factor (SIF), K_I (MPa√m)	Yield Stress, σys (Mpa)	Critical Stress Intensity Factor, K_{IC} (MPa√m)	Kr	1r	Load Factor or Factor of Safety	Crack Status
27	7.5	32.72	2.57	118.21	246.73	0.0104	0.2768	4.335	Stable
27	10	43.64	3.43	118.21	246.73	0.0139	0.3692	3.250	Stable
27	20	87.27	6.86	118.21	246.73	0.0278	0.7383	1.625	Stable
27	30	130.91	10.29	118.21	246.73	0.0417	1.1074	1.083	Stable
27	40	174.55	13.73	118.21	246.73	0.0556	1.4766	0.813	Failure
27	50	218.18	17.16	118.21	246.73	0.0695	1.8457	0.650	Failure
27	60	261.82	20.59	118.21	246.73	0.0835	2.2149	0.542	Failure
27	70	305.45	24.02	118.21	246.73	0.0974	2.5840	0.464	Failure
27	80	349.09	27.45	118.21	246.73	0.1113	2.9531	0.406	Failure
27	90	392.73	30.88	118.21	246.73	0.1252	3.3223	0.361	Failure

Initiation Point (Lr , Kr) = (1.2 , 0.04)

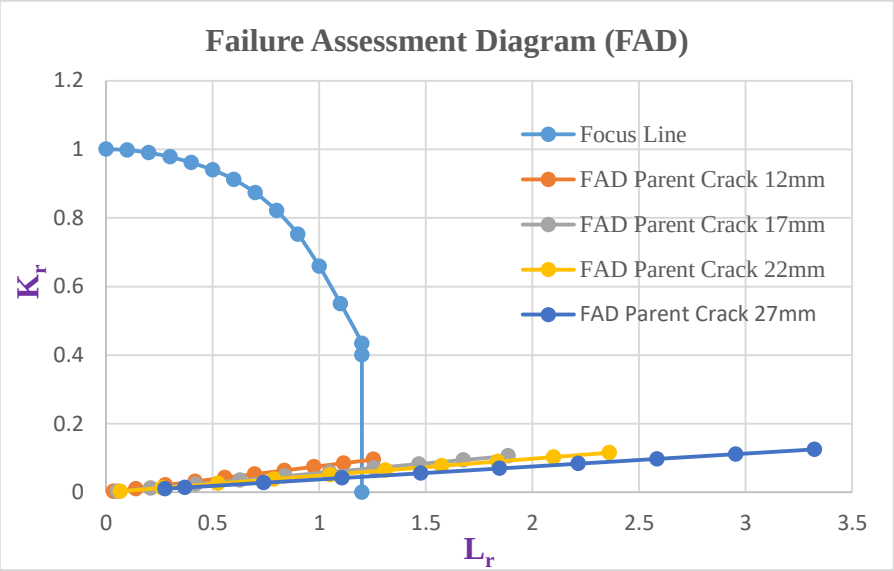

Figure 9: Failure Assessment Diagram (FAD) for Combined Parent Crack Length 12 mm, 17 mm, 22 mm and 27 mm

5. CONCLUSION

The fitness for service for crack of length 12 mm, 17 mm, 22 mm and 27 mm of API 5LX70 steel was investigated using the Failure Assessment Diagram (FAD). In developing and analysing the FAD, charpy V-notch impact test, monotonic tensile test and scanning electron microscopy were conducted. The energy result obtained from the charpy V-notch impact test was correlated numerically according to BS 7910 – 13 to obtain the critica1 stress intensity factor (K_Q) that was used alongside the stress intensity factor to generate the brittle fracture ratio $K_r = (K_I/K_Q)$ used as part of the parameters in the development of the FAD. Also, the reference stress that was obtained numerically also according to BS 7910 – 13 was used alongside the yield stress to generate the plastic collapse ratio ($L_r = \sigma_{ref}/\sigma_{ys}$) that was used in developing the FAD. The resu1ts show that the safe operational stress decreases with increase in crack length. It was observed that ductile fracture behaviour was suggested in the FAD analysis since the FAD graph falls within the plastic collapse zone of the FAD focus line and this was confirmed with the ductile fracture behaviour obtained from the SEM images. The study provided a novel way of establishing a standard for conducting fitness for services on API 5LX70 steel that is majorly used for pipeline. The failure assessment diagram (FAD) model can be used to properly schedule the rate of inspections on the pipeline to ascertain the safety of the pipeline alongside other inspection methods like Ultrasonic sound, radiographic, liquid penetrant and magnetic particle methods.

REFERENCES

[1] Leonardo, B. G., Luiz, C. C., Rodrigo, V. B. T. & Luiz, H. S. B. (2014). Microstructure and Mechanical Properties of Two API Steels for Iron Ore Pipelines, *Material Research.* 1-5. https://doi.org/10.1590/S1516-14392014005000068

[2] Maslat, S. A. (2006). Chloride Pitting Corrosion of API X80 and API X 100 High [Master's Thesis, University of British Columbia], 3(8), 25 – 26

[3] Suah, Y. (2014). Corrosion Behaviour of Low Carbon Steel used in Oil and Gas Aboveground Storage Tanks [Master's Thesis, African University of Science and Technology, 1(3), 2-9

[4] NACE International. (2016). The International Measures of Prevention, Application and Economics of Corrosion Technology *(IMPACT).* Houston: NACE International, 6, 1-5

[5] Obike, A. I., Uwakwe, K. J., Abraham, E. K., Ikeuba, A. I., & Emori, W. (2020). Review of the losses and Devastationcaused by Corrosion in Nigeria Oil Industry for over 30 years. *International Journal Corrosion Scale inhib*, 9(1) 74-91, https://doi.org/10.17675/2305-6894-2020-9-1-5

[6] Baorong, H., Xiaogang, L., Xiumin, M., Cuiwei, D., Dawei, Z., Meng, Z., Weichen, X., Dongzhu, Lu., & Fubin, M. (2017).The Cost of Corrosion in China, *nature partner journal*, 1(4), https://doi.org/10.1038/s41529-017

[7] Akinyemi, O. O., Nwaokocha, C. N., and Adesanya, A. O. (2012). Evaluation of Corrosion Cost of Crude Oil ProcessingIndustry. *Journal of Engineering Science and Technology*, 7(4), 517 – 528.

[8] British Standards Institution. (2013). Guide to methods for assessing the acceptability of flaws in metallic structures. London: BSI Group, 129 – 352.

[9] Tipple, C. & Thorwald, G. (2012). Using the Failure Assessment Diagram Method with Fatigue Crack Growth to Determine Leak before Rupture . *SIMULIA Customer Conference*, Boston: Quest Integrity Group, LLC, 2(1), 1-15.

[10] Zargarzadeh, P. (2013). Structural Integrity of CO2 Transportation Infrastructures, PhD Thesis, Cranfield University, UK. Bedford, 25-56.

[11] Hasanaj, A., Gjeta, A., & Kullolli, M. (2014). Analysing Defects with Failure Assessment Diagram of Gas Pipeline. *International Journal of Mechanical and Mechatronics Engineering*, 8(5), 1045 – 1047.
[12] ASTM International. (2013). Standard Test Methods for Measurement of Fatigue Crack Growth Rate. *ASTM International*, 6(3), 1 – 49. http://doi.org/10.1520/E0647-13A
[13] ASTM International. (2002). Standard Test Methods for Crack-Tip Opening Displacement (CTOD) Fracture Toughness Measurement. *ASTM International*, 3(1), 1 – 13
[14] ASTM International. (2012). Standard Test Method for Linear-Elastic Plane-Strain Fracture Toughness Ic of Metallic Materials. *ASTM International*, 1(2), 1 – 32
[15] Roylance, D. (2001). Mechanics of Material - Introduction to Fracture Mechanics. Cambridge: Massachusetts Institute of Technology
[16] Anderson, T. L (2017). Fracture Mechanics – Fundamental and Application. Boca Raton: CRC Press, 4, 8 – 150, https://doi.org/10.1201/9781315370293
[17] Marchi, C. S. & Somerday, B. P. (2023). Technical Reference on Hydrogen Compatibility of Materials. *Sandia National Laboriatories*, 1(3), 1 – 9.
[18] Murakami, Y. (1992). Stress Intensity Factors Handbook. Oxford: Pergamon Press, 2, 7 – 1
[19] Pilkey, W. (2004). Formula for Stress, strain and Structural Matrices. New Jersey: John Wiley & Sons, 5 – 8
[20] Yang, S. T. (2012). Stress Intensity Factor for High Aspect Ratio Semi-Elliptical Internal Surface Cracks in Pipes. *International Journal of Pressure Vessels and Piping*, 6(5), 13-23.
[21] ASTM International. (2013). Standard Test Method for Measurement of Fracture Toughness. West Conshohocken: ASTM International, 14 – 19.
[22] Hou, Y. L. (2016). Experimental Investigation on Corrosion Effect on Mechanical Properties of Buried Metal Pipes. *International Journal of Corrosion*, 9(8), 1-12.
[23] British Standards Institution. (2005). Fracture Mechanics Toughness Tests – Methods for determination of fracture toughness of metallic materials at rates of increase in stress intensity factor greater than 3.0MPa.m^0.5s^-1. London: BSI Group 15 – 20.